A Hybrid Electrochemical/Chemical Synthesis of Supported, Luminescent Cadmium Sulfide Nanocrystals

M. A. Anderson, S. Gorer, and R. M. Penner*

Institute For Surface and Interface Science, Department of Chemistry, University of California, Irvine, California 92679-2025

Received: February 20, 1997; In Final Form: May 12, 1997[⊗]

A hybrid electrochemical/chemical (E/C) method is employed to synthesize epitaxially oriented CdS nanocrystallites—size selectively—on graphite surfaces. The E/C synthesis involves three steps: (1) cadmium metal nanocrystals (NCs) are electrochemically deposited on the graphite basal plane surface; (2) cadmium NCs are oxidized at high pH to $Cd(OH)_2$; (3) upon immersion of the $Cd(OH)_2$ NCs in an aqueous sulfide solution, displacement of OH^- by S^{2-} occurs yielding wurtzite phase NCs of the semiconducting salt, cadmium sulfide. Dispersions of E/C-synthesized CdS nanocrystallites having mean diameters ranging from 20 to 80 Å were prepared and characterized using noncontact scanning force microscopy, transmission and high-resolution electron microscopy, selected area electron diffraction, and micrometer-scale spatially resolved photoluminescence spectroscopy. It is demonstrated that individual CdS nanocrystals are oriented with the *c*-axis of the crystallite perpendicular to basal plane (i.e. (0001)), and NCs located within the boundaries of a single grain on the graphite basal plane possess identical azimuthal orientations. Photoluminescence spectra reveal transitions that are assigned to band gap and surface trap states.

I. Introduction

To date, most experimental data pertaining to the electronic properties of semiconductor nanocrystals (NCs) has been obtained via spectroscopic investigations of *suspensions* of NCs in low-viscosity liquids,[1−9] silica glasses,[10−12] polymer matrices,[13−16] salt crystals,[17−19] and matrices prepared by sol−gel techniques.[20−22] But while suspensions of semiconductor NCs are convenient for optical investigations, future technological applications are likely to require the immobilization of NCs on the surfaces of conductors or semiconductors. Previously, this immobilization has been accomplished using either of two strategies: the *transferal of solution phase synthesized semiconductor NCs to a surface* or the *direct surface synthesis* of semiconductor NSc. The latter case, surface synthesis, has frequently involved the deposition of a material using either molecular beam epitaxy (MBE) or chemical vapor deposition (CVD). MBE has been employed, for example, to grow InAs islands on GaAs[23] and InP islands on GaInP,[24] whereas SiGe islands have been obtained using CVD on Si.[25,26] In general, the lateral dimension of the NCs obtained using MBE or CVD for a particular system (consisting of the deposited material and the surface) is not adjustable because it is determiend by the interfacial strain existing between the deposited material and the substrate surface lattice. The epitaxial electrochemical deposition of semiconductor nanocrystallites has recently been accomplished for the first time by Hodes, Rubinstein, and co-workers.[27,28] These workers have epitaxially grown high-quality, wurtzite CdSe nanocrystallites on Au(111) surfaces by galvanostatic deposition. Like MBE-based syntheses, it has been demonstrated that the interfacial strain energy determines the nanocrystallite diameter.[27,29]

Recently[30] we have reported that NCs of the I−VII semiconductor copper iodide (CuI) can be epitaxially grown on graphite surfaces using a completely new strategy involving three steps: (1) electrochemical deposition of copper NCs, (2) electrochemical oxidation of these NCs to Cu_2O, and (3) displacement of O^{2-} by I^- to yield β-CuI NCs. This electrochemical/chemical hybrid procedure (henceforth E/C) yielded CuI NCs having mean diameters in the range from 13 to 100 Å, and these graphite-supported NCs exhibited strong, room temperature luminescence consistent with a transition across the band gap of this material and a "strong" quantum size effect.[30]

SCHEME 1: Schematic Diagram Illustrating the Three-Step Electrochemical/Chemical (E/C) Synthesis of Expitaxial CdS Nanocrystals

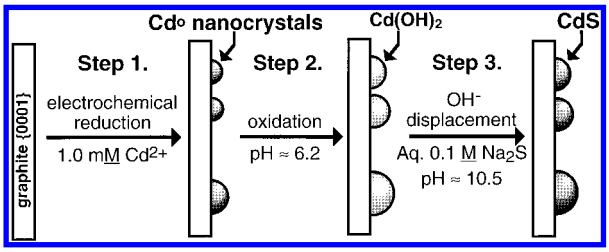

In this Letter, we describe an E/C scheme for the synthesis of CdS NCs on the graphite basal plane surface. Using selected area electron diffraction, the intermediates involved in the synthesis are identified, it is demonstrated that CdS NCs are epitaxially aligned with the graphite surface, and the orientation of the wurtzite CdS unit cell on the graphite surface is specified. It is further shown that E/C-synthesized CdS NCs are strongly photoluminescent (PL) at room temperature with both blue-shifted band gap and trap state emissions present in PL spectra; a complete study of the PL from E/C-synthesized CdS nanocrystals as a function of size will be presented in a future publication. The demonstration of an E/C synthesis for CdS NCs also suggests that the E/C method is significantly general; permitting the preparation of both I−VII (e.g. CuI) and II−VI (e.g. CdS) materials.

II. Materials and Methods

The E/C synthesis of CdS nanocrystals, shown in Scheme 1, is a three-step processes analogous to the procedure recently

* Address correspondence to this author at rmpenner@uci.edu.
⊗ Abstract published in *Advance ACS Abstracts,* July 1, 1997.

S1089-5647(97)00627-5 CCC: $14.00

employed to synthesis CuI NCs:[30] (1) Cd° NCs which are narrowly dispersed in size are electrochemically deposited from an aqueous 1.0 mM CdF_2: 0.1 M NaF (pH ≈ 6.2) plating solution onto a freshly cleaved graphite basal plane surface; (2) Cd° NCs spontaneously oxidize in this plating solution at open circuit (and in the pH = 10.5, 0.1 M Na_2S solution, *vide infra*); (3) the graphite surface is removed from the electrochemical cell, and air-stable $Cd(OH)_2$ NCs are then immersed in an aqueous 0.1 M Na_2S solution (pH ≈ 10.5) in which the displacement of OH^- by S^{2-} occurred in 1 min. Selected area electron diffraction analyses (*vide infra*) confirm that wurtzite CdS NCs having a mean diameter of 20−80 Å were thereby obtained. As in the case of CuI, the size and size monodispersity of the CdS NCs prepared by the E/C method are determined by the corresponding properties of the Cd° NCs that are deposited in step 1.

Further details regarding the pulsed, overpotential deposition (pulsed OPD) of Cd° (step 1) are as follows: a platinum wire counter electrode and mercurous sulfate (MSE) reference electrodes were employed; a deposition overpotential of −350 mV (vs the reversible Nernst potential for 1.0 mM Cd^{2+}/Cd°) was used; current transients for the deposition of cadmium metal were corrected for background non-Faradaic current. The procedures for transmission electron microscopy (TEM), selected area electron diffraction (SAED), noncontact atomic force microscopy (NC-AFM), and surface laser-induced fluorescence measurements were all as previously described.[30]

III. Results and Discussion

Previously we have described the electrochemical deposition of silver[31] and copper[30] NCs from dilute (≈1.0 mM) plating solutions on the graphite basal plane surface. On the basis of measurements of the current−time transients and *ex-situ* NC-AFM imaging of the graphite electrode surface following deposition, we concluded that for both metals deposition occurs via an instantaneous nucleation and radial diffusion-limited growth mechanism. As in this previous work, current−time transients for cadmium deposition increased in direct proportion to $t^{1/2}$ at short times (t < 30 ms) again consistent with an instantaneous nucleation and radial diffusion-limited growth mode for cadmium metal. Consistent with this hypothesis, NC-AFM images of graphite surfaces on which cadmium was first deposited and then oxidized (to $Cd(OH)_2$) revealed a dispersion of particles which, on average, were well separated from one another on atomically smooth regions of the surface. The particle areal density of $\approx 10^{10}$ cm^{-2} was also in the range seen for NCs of Ag° and Cu° prepared using pulsed OPD. These NC-AFM images (not shown) are qualitatively identical to those of CdS shown in Figure 2.

Graphite surfaces were analyzed by TEM and SAED twice: following the oxidation of cadmium and then following the exposure of the oxidized surface to Na_2S. Figure 1a shows a bright-field TEM image and Figure 1b,c the SAED pattern for a surface on which cadmium was deposited and subsequently oxidized. The TEM image reveals a 330 × 330 nm region of the surface. Within this region, ≈100 particles as small as ∼10 Å in diameter are visible. The SAED image of Figure 1b was obtained from a 10 μm diameter region, centered on the area displayed in 1a, and encompassing hundreds of particles. In addition to the graphite diffraction spots, three diffuse rings are visible in this diffraction pattern with reciprocal spacings consistent with powder diffraction data for $Cd(OH)_2$ (XRD file No. 31-0228), as shown in the assignment of Figure 1c. Only [100], [110], and [200] diffractions are seen for $Cd(OH)_2$ NCs, while [001] and [101] are missing. This suggests that wurtzite $Cd(OH)_2$ NCs are oriented with the *c*-axis of the unit cell perpendicular to the surface, although these NCs clearly possess no preferred azimuthal orientation.

A different region of the same surface is shown in the TEM image of Figure 1d. Here, particles are larger with diameters in the range from 60 to 80 Å, and the corresponding diffraction pattern (Figure 1e) shows [100] and [200] single-crystal diffractions assignable (Figure 1f) to FCC cadmium metal (XRD file No. 05-0674). While just two pairs of diffraction spots for Cd are seen in the pattern of Figure 1e, all six spots for each of the first two orders were observed by tilting the specimen stage in the TEM slightly. In other SAED measurements of oxidized surfaces following cadmium deposition, it was generally observed that regions in which exclusively small particles (diameter < 20 Å) were present yielded powder patterns assignable to $Cd(OH)_2$, whereas regions encompassing mostly particles larger than 40−50 Å were associated with single-crystal FCC cadmium diffraction. Under the oxidation conditions employed here, then, we conclude that the smaller Cd° NCs oxidize more readily and that this oxidation destroys the azimuthal alignment of cadmium metal nanocrystals with the surface.

TEM and SAED analysis of a region of the same surface following immersion in aqueous Na_2S is shown in Figure 1g−i. The region shown is exactly the same one seen in Figure 1d−f, and many of the same particles with virtually the same shape and size are discernable. The SAED pattern from this region (Figure 1f) again shows single-crystal diffraction; however, the *d* spacing of the spots are consistent with [100] and [200] for wurtzite phase CdS (file No. 41-1049). In other regions of the surface where smaller $Cd(OH)_2$ NCs had been found by SAED immediately after oxidation, the diffuse rings seen for $Cd(OH)_2$ were also replaced by single-crystal diffraction spots corresponding to [100] and [200] for CdS. In other words, epitaxial CdS NCs were obtained both at regions of the surface where electrochemical oxidation yielded epitaxial Cd° and at regions where only nonepitaxial $Cd(OH)_2$ NCs were present. The orientation of CdS NCs on the graphite surface may be deduced from the electron diffraction pattern as follows: diffractions corresponding to periodicities existing along the *c*-axis of the unit cell (e.g., [001] and [002]) are missing, whereas the strongest diffraction spot (i.e. [100]) corresponds to a 3.58 Å periodicity existing within hexagonal cadmium or sulfide layers in the wurtzite structure. Together, these two observations indicate that the *c*-axis of CdS nanocrystals is oriented perpendicular to the plane of the graphite surface and that hexagonal planes of either cadmium or sulfur atoms—with a lattice constant of a = 4.14 Å—are in contact with the graphite surface. The overlayer structure consistent with the diffraction data is shown in the schematic diagram of Figure 1j. This structure also corresponds to the global energy minimum on the basis of calculations for the wurtzite CdS lattice on the hexagonal graphite surface and corresponds to a unit cell misfit of ∼3%.[32]

This result—in particular the existence of a cadmium metal intermediate—is apparently inconsistent with the mechanism for the E/C synthesis postulated earlier[30] (and depicted in Scheme 1), which required the presence of an intermediate oxide in which the metal was present in the correct oxidation state for conversion to the semiconducting salt. We therefore investigated the possibility that further oxidation of the metal intermediate to an oxide occurred (at open circuit) upon the immersion of cadmium metal NCs into the pH = 11 Na_2S solution. SAED data for 10−80 Å Cd° NCs that were immersed in aqueous, pH = 11 KOH solutions indicated $Cd(OH)_2$ powder diffraction patterns similar to those seen for smaller particles after electrochemical oxidation (data not shown). We therefore

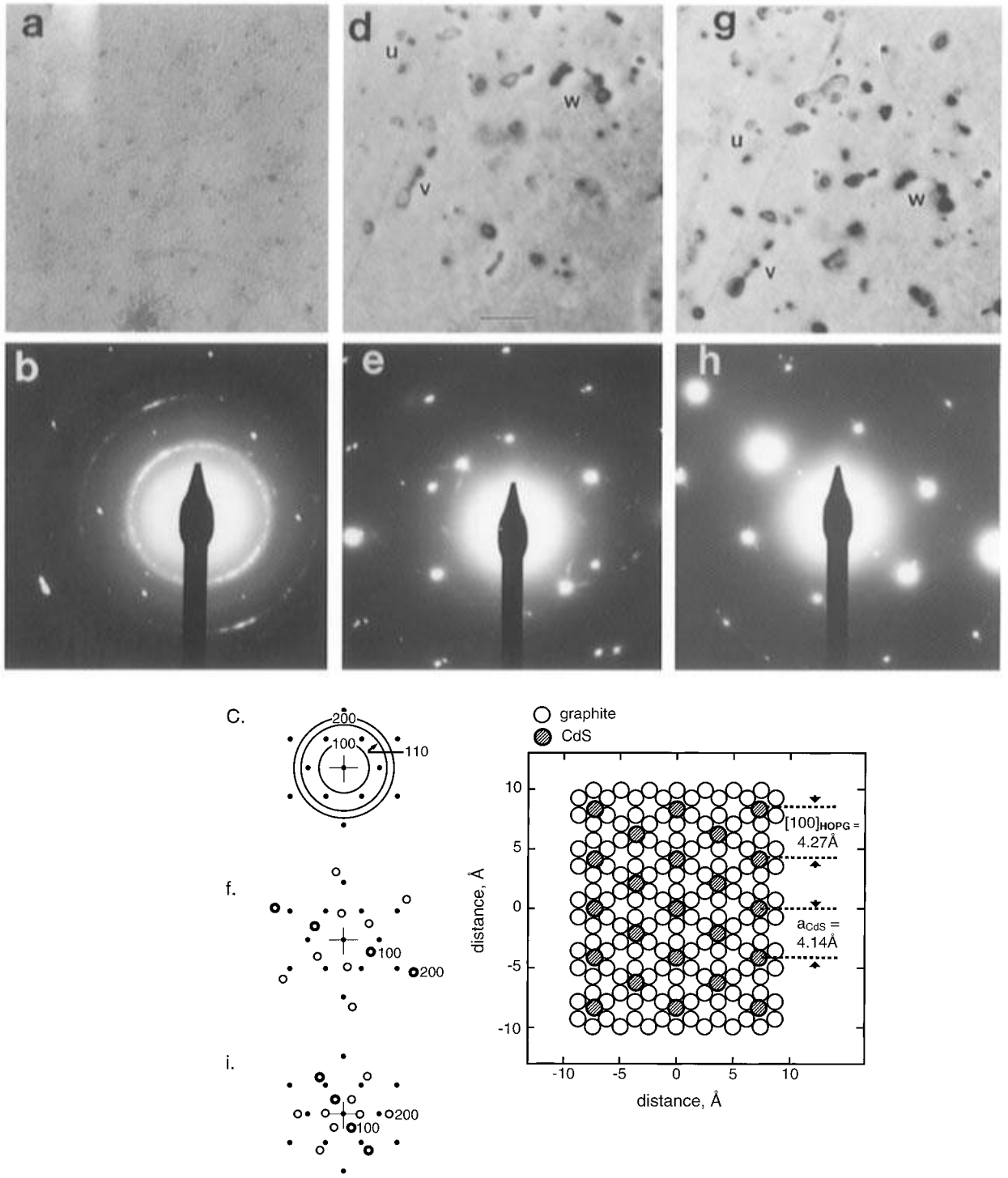

Figure 1. Transmission electron micrographs and selected area electron diffraction (SAED) data for oxidized cadmium NCs (a−f) and CdS NCs (g−i). The distance bar shown is the same for all TEM images and corresponds to 80 nm. (a) Transmission electron micrograph (TEM) of an electron-transparent graphite surface immediately following the electrochemical deposition of Cd and oxidation to $Cd(OH)_2$. (b) SAED analysis of a 10 μm diameter region centered about the TEM image of (a). (c) Schematic diagram of the SAED pattern of (b) showing assignments. The rings correspond to [100], [110], and [200] of $Cd(OH)_2$ (XRD file No. 31-0228); solid circles correspond to [100] and [110] of HOPG (XRD file No. 41-1487). (d) TEM image of other area of the same sample. Lower case letters u, v, and w indicate distinctive clusters of nanocrystallites. (e) SAED analysis of a 10 μm diameter region centered about the TEM image of (d). (f) Schematic diagram of the SAED pattern of (e) showing assignments. The open circles correspond to [100] and [200] of FCC Cd metal (XRD file No. 05-0674); solid circles correspond to [100] and [110] of HOPG (XRD file No. 41-1487). (g) TEM image of the same region shown in (d) but following the immersion of the surface in aqueous 0.10 M Na_2S solution for 60 s. The lower case letters letters u, v, and w indicate the same clusters of NCs marked in (d). (h) SAED analyses of a 10 μm diameter region centered about the TEM image of (g). (i) Schematic diagram of the SAED pattern of (h) showing assignments. The open circles correspond to [100] and [200] of wurtzite phase CdS (XRD file No. 41-1049); solid circles correspond to [100] and [110] of HOPG (XRD file No. 41-1487). (j) Schematic diagram of the orientation of hexagonal cadmium (or sulfur) layers of the wurzite CdS nanocrystals on the graphite surface as indicated by the electron diffraction data.

postulate that a Cd^{II}hydroxide intermediate is obtained prior to conversion to CdS also for larger Cd° NCs.

Noncontact atomic force microscopy images of a typical graphite surface following E/C synthesis of CdS NCs are shown in Figure 2. In this instance, 75.2 μC cm^{-2} was deposited, corresponding to 0.12 equiv. cadmium atomic layers. Well-separated, CdS NCs with heights of ≈10 Å are evident in this image. The width of these particles appears to be approximately

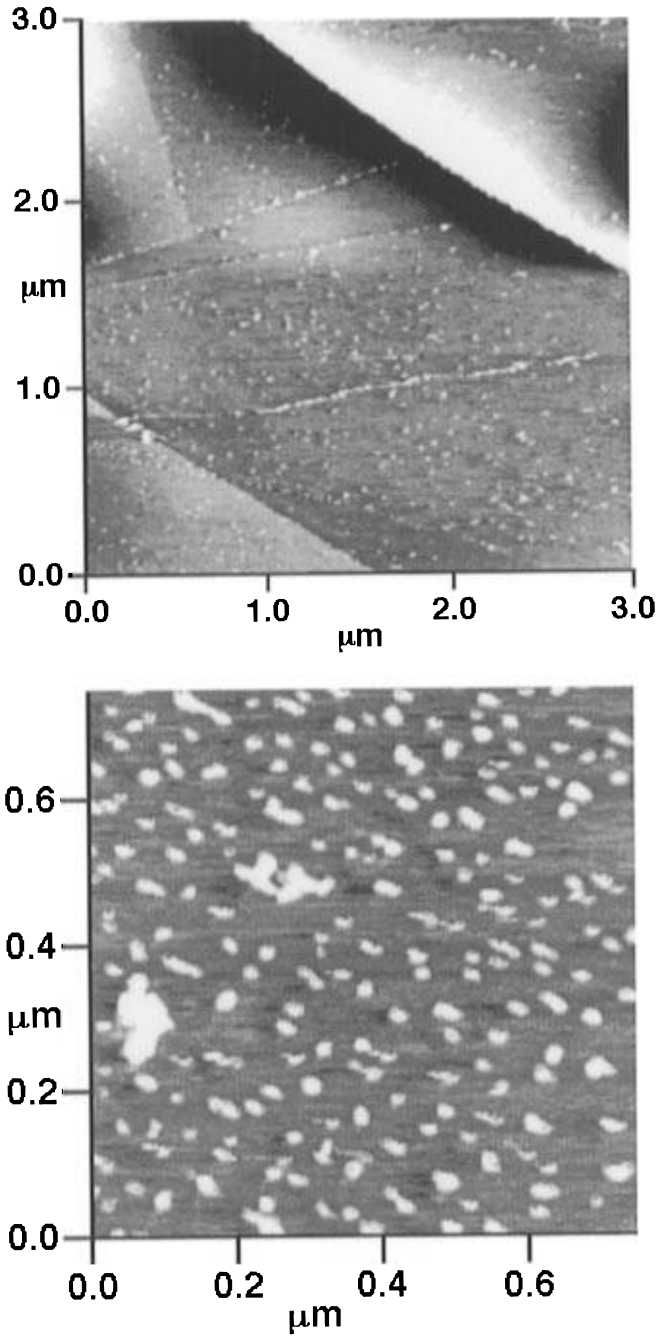

Figure 2. Noncontact atomic force microscope images of CdS NCs prepared with a cadmium plating duration of 150 ms, which yielded 75.2 μC cm^{-2} of cadmium metal: (A, top) 3.0 μm × 3.0 μm image; (B, bottom) 0.8 μm × 0.8 μm image.

10 times the height; however, this broadening is an artifact of the convolution of the AFM tip geometry with that of the nanocrystallite and has been seen in previous investigations of metal[31,33] and CuI nanocrystals.[30] The maximum particle height is not affected by this tip convolution effect. Histograms of particle height for two different samples of CdS NCs are shown in Figure 3. As seen in the histogram of Figure 3a, good particle size monodispersity (RSD ≈ 30%) is usually obtained for small CdS NCs, having a diameter of less than 20 Å. Particle size distributions for samples having a mean diameter >40 Å were typically much broader. In fact, the particle size distribution for such preparations is frequently bimodal, as seen in the histogram of Figure 3b. The development of this polydispersity for large nanocrystals is incompletely understood at present.

CdS nanocrystals prepared by the E/C method exhibit strong, room temperature photoluminescence (PL) spectra even in a laboratory air ambient. A typical spectrum, shown in Figure

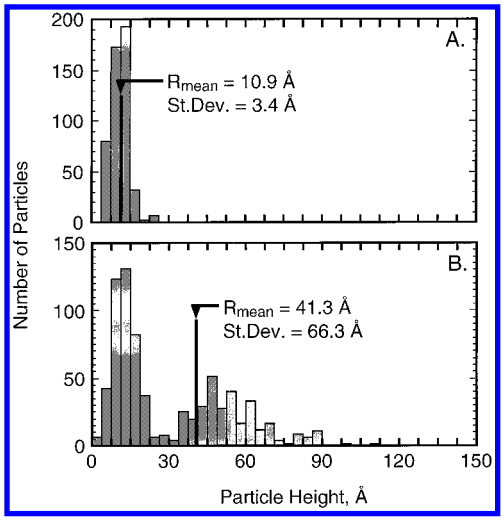

Figure 3. Histograms of two surfaces on which CdS NCs were deposited: (A) 75.2 μC cm^{-2} cadmium metal deposited in a 150 ms pulse; (B) 550 μC cm^{-2} cadmium metal deposited in a 1.0 s pulse.

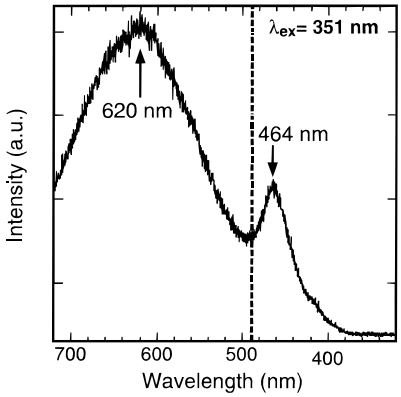

Figure 4. Photoluminescence spectrum obtained from a 30 μm diameter region of a CdS NC-covered graphite surface at room temperature. This sample was prepared using an initial cadmium energy coverage at ≈500 μC cm^{-2} obtained using a 1.0 s deposition pulse duration.

4, exhibits two maxima: At low energies, a broad transition having a maximum at ≈620 nm (or in general 600−650 nm) and a narrower emission peak centered at 464 nm (or 440−465 nm). The broader peak in the red is assigned to emission from trap states located in the "forbidden" region of the band gap. This peak is often the only transition seen in PL spectra of solution phase synthesized CdS NCs[3] and CdS thin films deposited by a variety of methods.[34,35] The peak at 464 nm, on the other hand, is assigned to band gap emission. This sample was similar to that of Figure 3b, and the 464 nm emission is significantly blue-shifted from macroscopic band gap of CdS (≈500 nm) in accordance with the expectations of the strong confinement model[36] and a particle diameter of 50 Å.[37] Previously, it has usually been necessary to saturate the surface states of solution phase synthesized CdS NCs using Lewis bases such as NH_3 in order to observe band gap emission.[38] The observation of this transition in as-synthesized CdS is an indication that the E/C method yields CdS NCs possessing an inherently low defect density.

IV. Summary

A hybrid E/C method has been developed for the synthesis of CdS NCs having mean diameters in the range from 20 to 100 Å on graphite surfaces. The E/C synthesis involves the electrodeposition of Cd° NCs, the conversion of these NCs to $Cd(OH)_2$, and finally the displacement of OH^- by S^{2-}. The

resulting CdS NCs are epitaxially aligned with the hexagonal periodicity of the graphite surface, are strongly luminescent, and, for NC samples with mean diameters below 40 Å, are narrowly dispersed in size.

Acknowledgment. The authors express their appreciation to Dr. Art Moore of Advanced Ceramics for donations of highly oriented pyrolytic graphite, to Prof. John Hemminger and graduate student Mickey Laux for performing the XPS measurements, and to Prof. Hemminger for helpful discussions. This work was supported by the Office of Naval Research (N00014-93-0757) and the NSF Yound Investigator's Program (DMR-9257000). In addition, the following are gratefully acknowledged: a Department of Education GAANN Fellowship (M.G.A.), a Welch Scholarship of the International Union for Vacuum Science (S.G.), and an A.P. Sloan Fellow, an Arnold and Mabel Beckman Young Investigator award, and a Camille Dreyfus Teacher-Scholar award (R.M.P.).

References and Notes

(1) Dance, I. G.; Choy, A.; Scudder, M. L. *J. Am. Chem. Soc.* **1984**, *106*, 6285.
(2) Brus, L. E. *J. Phys. Chem.* **1986**, *90*, 225.
(3) Herron, N.; Wang, Y.; Eckert, H. *J. Am. Chem. Soc.* **1990**, *112*, 1322.
(4) Johansson, K. P.; McLendon, G.; Marchetti, A. P. *Chem. Phys. Lett.* **1991**, *179*, 321.
(5) Tricot, Y.-M.; Fendler, J. H. *J. Am. Chem. Soc.* **1984**, *90*, 3369.
(6) Mulvaney, P. *Colloids Surf. A* **1993**, *81*, 231.
(7) Micic, O. I.; Meglic, M.; Lawless, D.; Sharma, D. K.; Serpone, N. *Langmuir* **1990**, *6*, 487.
(8) Steigerwald, M. L.; Alivisatos, A. P.; Gibson, J. M.; Harris, T. D.; Kortan, R.; Muller, A. J.; Thayer, A. M.; Duncan, T. M.; Douglass, D. C.; Brus, L. E. *J. Am. Chem. Soc.* **1988**, *110*, 3046.
(9) Uchida, H.; Curtis, C. J.; Kamat, P. V.; Jones, K. M.; Nozik, A. J. *J. Phys. Chem.* **1992**, *96*, 1156.
(10) Ekimov, A. I.; Efros, A. L.; Onushchenko, A. A. *Solid State Commun.* **1985**, *56*, 921.
(11) Dvorak, M. D.; Justus, B. L.; Gaskill, D. K.; Hendershot, D. G. *Appl. Phys. Lett.* **1995**, *66*, 804.
(12) Masumoto, Y.; Kawabata, K.; Kawazoe, T. *Phys. Rev. B* **1995**, *52*, 7834.
(13) Dabbousi, B. O.; Bawendi, M. G.; Onitsuka, O.; Rubner, M. F. *Appl. Phys. Lett.* **1995**, *66*, 1316.
(14) Salata, O. V.; Dobson, P. J.; Hull, P. J.; Hutchison, J. L. *Appl. Phys. Lett.* **1994**, *65*, 189.
(15) Noglik, H.; Pietro, W. J. *Chem. Mater.* **1995**, *7*, 1333.
(16) Wang, Y.; Herron, N. *Phys. Rev. B* **1990**, *42*, 7253.
(17) Masumoto, Y.; Wamaura, T.; Iwaki, A. *Appl. Phys. Lett.* **1989**, *55*, 2535.
(18) Wamura, T.; Masumoto, Y.; Kawamure, T. *Appl. Phys. Lett.* **1991**, *59*, 1758.
(19) Itoh, T.; Iwabuchi, Y.; Kirihara, T. *Phys. Status Solidi B* **1988**, *146*, 531.
(20) Spanhel, L.; Anderson, M. A. *J. Am. Chem. Soc.* **1991**, *113*, 2826.
(21) Zhang, Y.; Raman, N.; Bailey, J. K.; Brinker, C. J. *J. Phys. Chem.* **1992**, *96*, 9098.
(22) Choi, K. M.; Hemminger, J. C.; Shea, K. J. *J. Phys. Chem.* **1995**, *99*, 4720.
(23) Marzin, J.-Y.; Gerard, J.-M.; Izrael, A.; Barrier, D.; Bastard, G. *Phys. Rev. Lett.* **1994**, *73*, 716.
(24) Castrillo, P.; Hessman, D.; Pistol, M.-E.; Anand, S.; Carlsson, N.; Seifert, W.; Samuelson, L. *Appl. Phys. Lett.* **1995**, *67*, 1905.
(25) Apetz, R.; Vescan, L.; Hartmann, A.; Dieker, C.; Luth, H. *Appl. Phys. Lett.* **1995**, *66*, 445.
(26) Schittenhelm, P.; Gail, M.; Brunner, J.; Nutzel, J. F.; Abstreiter, G. *Appl. Phys. Lett.* **1995**, *67*, 1291.
(27) Golan, Y.; Ter-Ovanesyan, E.; Manassen, Y.; Margulis, L.; Hodes, G.; Rubinstein, I.; Bithell, E. G.; Hutchison, J. L. *Surf. Sci.* **1996**, *350*, 277.
(28) Golan, Y.; Margulis, L.; Hodes, G.; Rubinstein, I.; Hutchinson, J. L. *Surf. Sci.* **1994**, *311*, L633.
(29) Golan, Y.; Hodes, G.; Rubinstein, I. *J. Phys. Chem.* **1996**, *100*, 2220.
(30) Hsiao, G. S.; Anderson, M. G.; Gorer, S.; Harris, D.; Penner, R. M. *J. Am. Chem. Soc.* **1997**, *119*, 1439.
(31) Zoval, J. V.; Stiger, R. M.; Biernacki, P. R.; Penner, R. M. *J. Phys. Chem.* **1996**, *100*, 837.
(32) Energy minimization calculations were performed as follows: The minimum energy spacing between a two-layer thick graphite {0001} surface and a two-layer thick wurtzite CdS nanocrystal was located for various orientations of the CdS nanocrystal on the graphite surface. For each orientation, the energy was calculated as the sum of the pairwise interaction forces integrated from a large separation (10 Å). In all cases, [111] planes of the CdS nanocrystal were constrained to be parallel to the graphite surface. A Lennard-Jones potential parameterized for argon or neon was employed for these calculations; the orientation of the CdS NC corresponding to the global minimum was not sensitive to the parameterization of the potential.
(33) Zoval, J. V.; Biernacki, P.; Penner, R. M. *Anal. Chem.* **1996**, *68*, 1585.
(34) Chevreau, A.; Phillips, B.; Higgins, B. G.; Risbud, S. H. *J. Mater. Chem.* **1996**, *6*, 1643.
(35) Chestnoy, N.; Harris, T. D.; Hull, R.; Brus, L. E. *J. Phys. Chem.* **1986**, *90*, 3393.
(36) Brus, L. E. *J. Chem. Phys.* **1984**, *80*, 4403.
(37) CdS is a classical material for the demonstration of the strong quantum size effect. The exciton radius for CdS is 30 Å (see, for example: Yoffe, A. D. *Adv. Phys.* **1993**, *42*, 173), and the effective masses of electrons and holes are $m_h = 0.2m_e$, $m_h = 0.7m_e$ (Pankove, J. I. *Optical Processes in Semiconductors*; Dover Publication, Inc: New York, 1975).
(38) Henglein, A. *Chem. Rev.* **1989**, *89*, 1861.